agriculture

MDPI

Article

Design and Test of Single-Disc Opener for No-Till Planter Based on Support Cutting

Guangyuan Zhong [1,2], Hongwen Li [1,2,*], Jin He [1], Qingjie Wang [1], Caiyun Lu [1], Chao Wang [1], Zhenwei Tong [1], Dandan Cui [1] and Dong He [1]

[1] College of Engineering, China Agricultural University, Beijing 100083, China
[2] Key Laboratory of Agricultural Equipment for Conservation Tillage, Ministry of Agricultural and Rural Affairs, Beijing 100083, China
* Correspondence: lhwen@cau.edu.cn; Tel.: +86-010-6273-7300

Abstract: To solve the problem of low straw-cutting efficiency of single-disc openers of no-till planters under conditions of high soil moisture content, a single-disc furrowing and straw-cutting device was designed based on the support-cutting principle. To improve the straw-cutting ability of the disc opener when it operates under high-moisture-content soil conditions and to make sure that the straw that is not cut by the disc coulter can be cut smoothly by the disc opener, the support shovel was designed, and the operation mechanism of the support shovel device was analyzed. The soil moisture content, the support shovel's entry angle, the support shovel's entry gap angle, and the support shovel's tip margin were identified as the factors influencing the device design through the theoretical analysis of the furrowing and straw-cutting device. Through the discrete element method (DEM), a single-factor simulation test was first conducted to analyze how different soil moisture contents affected the device's ability to cut straw, and the results showed that the number of broken bonds was lowest when the soil moisture content was 20 ± 1%, and the time taken for the straw to be wholly cut off was also the longest. Then, a quadratic orthogonal simulation test was conducted to construct a regression model and optimize the parameters at the soil moisture content of 20 ± 1%, and the results revealed that the significant order of each factor's influence on the number of broken bonds is as follows: entry gap angle, entry angle, and shovel tip margin. In addition, the device's overall operation quality was better when the entry angle was 49°, the entry gap angle was 0°, and the shovel tip margin was 10 mm. At this time, the number of broken bonds was predicted to be 506. Finally, the simulation validation test was run, and the number of broken bonds was obtained to be 478, with a relative error of 5.6% from the predicted value. According to the optimal parameters to complete the device trial production and field test, the results show that the average cut-off rate of the device is 71.7%, the stability coefficient of the furrowing depth is 90.87%, and the performance of the furrow opening is excellent, which meets the requirements of a no-tillage seeding operation. This study can provide a reference for the design and improvement of no-tillage seeding machines under conditions of high soil moisture content.

Keywords: single-disc opener; support cutting; soil moisture content; discrete element method (DEM); parameter optimization

Citation: Zhong, G.; Li, H.; He, J.; Wang, Q.; Lu, C.; Wang, C.; Tong, Z.; Cui, D.; He, D. Design and Test of Single-Disc Opener for No-Till Planter Based on Support Cutting. *Agriculture* **2023**, *13*, 1635. https://doi.org/10.3390/agriculture13081635

Academic Editors: Mustafa Ucgul and Chung-Liang Chang

Received: 27 July 2023
Revised: 16 August 2023
Accepted: 17 August 2023
Published: 19 August 2023

1. Introduction

Conservation tillage improves soil organic matter, prevents wind erosion, and conserves moisture [1]. No-till seeding may significantly increase productivity while lowering labor expenses, and it has been extensively used in China [2]. In the two mature Huang-Huai-Hai wheat and maize regions, there is much maize straw during the wheat no-tillage seeding process. In the case of high soil moisture content, the stubble cutter at the front of the no-tillage planter cannot completely cut off the straw, while the traditional single-disc opener has a poor cutting effect, and the straw will block the planter and cause a high

seed-drying rate, which affects seed emergence [3]. Therefore, improving the straw-cutting ability of disc openers when operating under high-moisture-content soil conditions and ensuring that the straw not cut by the stubble cutter can be cut off by the disc opener is the key to solving the clogging of wheat no-till planters and improving the quality of seeding.

The traditional single-disc opener utilizes a disc with a slight angle to the direction of movement and a vertical direction to move the soil laterally to form a furrow [4]. Moreover, the disc has a certain ability to cut crop straw [5], and the cutting performance is affected by the different geometry of the disc and its operating parameters [6]. The shape of the disc has a significant impact on the straw-cutting effect [7,8]; at the same working depth, the cutting effect of ripple disc, notched disc, and plain disc decreases in order [9], but the disturbance width of the soil does increase accordingly [6]. Different disc diameters have different straw-cutting capacities [10], but the vertical force required increases with increasing diameter [11]. Insufficient downforce will cause the disc opener to push the incompletely cut straw into the seed furrow, which will cause "hair-pinning", suspend the seed, and hinder its emergence [12,13]. Increasing the downward pressure is more conducive to the cutting of straw [14]. Straw-cutting efficiency is also affected by the operating speed of the opener disc [15], and the efficiency of straw-cutting will be improved with an increase in the operating speed [16]. The disc angle and tilt angle are the most crucial factors in figuring out how well the openers will furrow and cut straw, and the large rake angle can promote the "hair-pinning" of residue in wet or soft soil conditions [17]. At the same time, increasing the disc angle decreases the specific draft, side, and vertical forces, and increasing the tilt angle causes the specific vertical, draft, and side forces to increase [18]. Existing research has focused on the effects of disc geometry and operating parameters on tillage performance but has not yet considered the impact of soil characteristics on the operational performance of single-disc openers.

To address the aforementioned problems, this study designs a furrow opener with a straw-cutting device based on the principle of support cutting to enhance the efficiency of straw that has not been cut off by the stubble cutter to be cut by the single-disc furrow opener under the condition of high soil moisture content, lessen "hair-pinning", and enhance the quality of seeding. The parameters of the device's essential components are established through theoretical analysis, the straw-cutting process is simulated by EDEM, the optimal structural parameter combination is established by the quadratic orthogonal combination test, and the optimized device is put through field tests to confirm its functionality.

2. Materials and Methods

2.1. Structure and Working Principle

2.1.1. Structure

The major components of the device are seen in Figure 1 and include a disc coulter, a scraper, a support shovel, a disc hanging plate, etc. The installation disc angle and tilt angle are both 0°; the scraper is positioned on one side of the disc and can scrape off the soil adhering to the disc as well as assist in the opening of furrows. The support shovel is positioned on the same side as the scraper and passes through the scraper; the disc can cut off the straw under the support provided by the support shovel and open the suitable seed furrow.

2.1.2. Working Principle

During the operation, the front end of the support shovel reaches into the soil with a certain entry angle, and with the forward movement of the machine, the soil is slightly raised by the support shovel. The disc coulter then cuts the soil, which is divided into two parts, completing the initial seed furrow guidance and forming the seed furrow prototype. The soil moves along the disc's sides on both sides, and under the scraper's compression and compacting action forces, soil on one of the disc's sides is pushed away and lifted, widening and stabilizing the narrow seed furrow into a complete seed furrow that satisfies

the requirements of agronomy. The scraper also has the function of scraping away the soil adhering to the disc while completing the furrow opening to prevent the furrow-opening disc from adhering to too much soil. Figure 2 depicts the changes in the soil that occur during the single-disc opener's soil-penetration procedure.

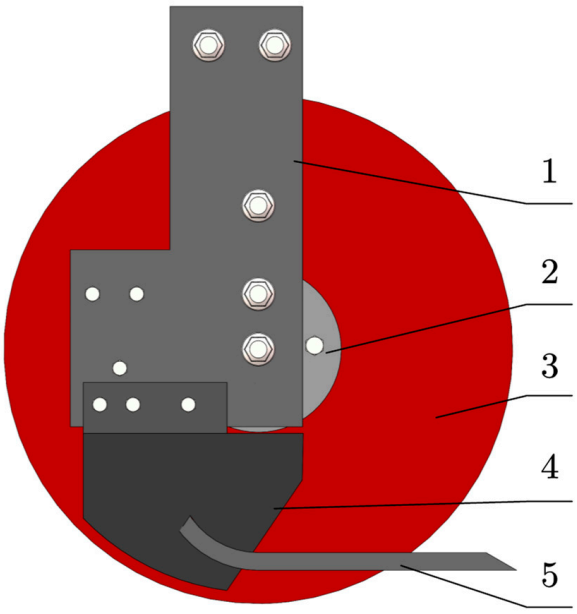

Figure 1. Schematics of opener structure: 1. disc hanging plate; 2. bearing base; 3. disc coulter; 4. scraper; 5. support shovel.

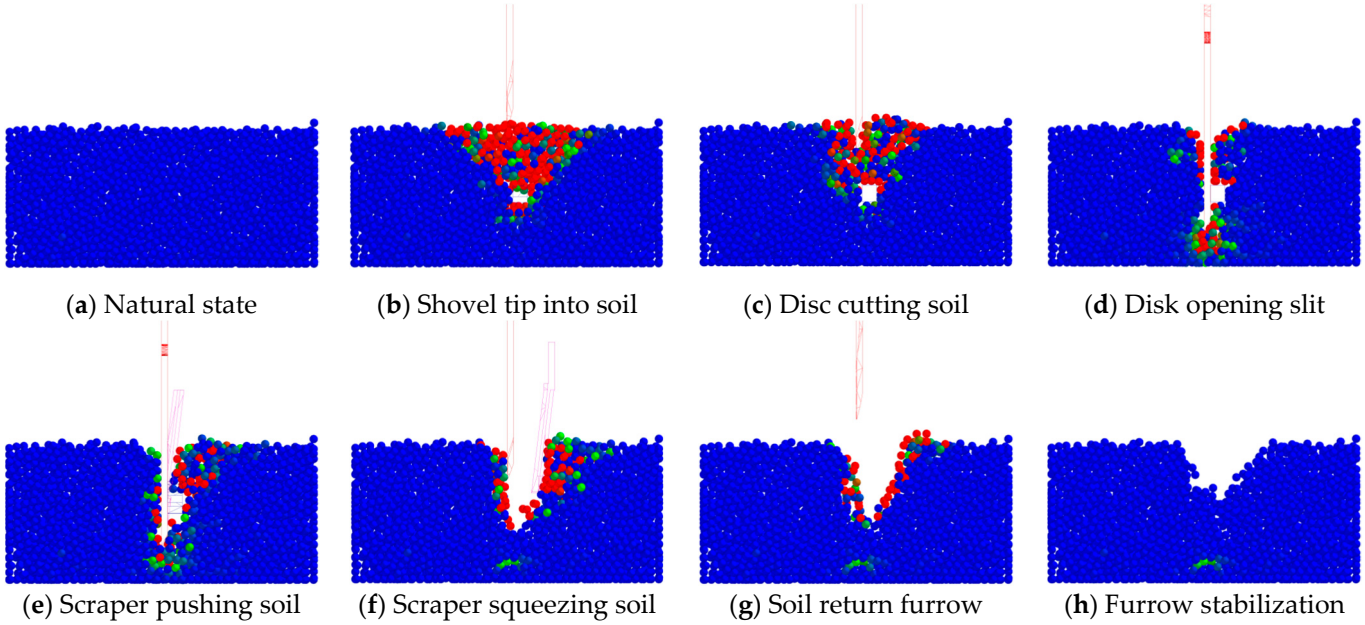

Figure 2. Single-disc opener entering the soil process.

When the opener has not penetrated the soil, the soil is in its natural state (Figure 2a). The support shovel penetrates the soil first; its tip slices the dirt, and the soil on its upper half has a tendency to move higher under its action (Figure 2b). With the advancement of the opener, the soil is warped. The disc cuts the warped soil from the top, and as the disc rotates, the soil is opened up to a slit (Figure 2c,d). The scraper pushes the soil on one side away from the slit and compacts it (Figure 2e,f), and the soil is piled up on one side.

The pile of soil particles begins to flow back into the seed furrow after the opener has left (Figure 2g) until the shape of the seed furrow is stabilized (Figure 2h).

2.2. Design of Key Components

The operating performance of the opener is mainly affected by factors such as the outside environment and its structural design. External factors include the physical and chemical properties of the soil, the operating speed of the machine, and the operating depth of the opener. Structural design factors are the shape of the support shovel, the diameter of the disc, and the shape of the scraper.

2.2.1. Analysis of Straw Forces

The ordinary single-disc coulter balances the disc's cutting force by using the soil's supporting force and the straw's bending resistance. Due to the straw's low stiffness, when the soil is soft, the straw's supporting force fluctuates with its depth, making it difficult to reach the force balance, difficult to cut off [11], and simple to press into the soil by the disc. The seeds are easily aerated by straw when sowing at this time. Increase the support shovel at the bottom so that when the straw penetrates the soil and reaches it, the support force is fixed and may be conducive to straw cutting. If the soil is loose, the disc drives the straw into the soil until it touches the support shovel at a distance of h from the furrow's bottom. Assume that the angle between the support shovel and the soil level is 0°. Use the straw as a mass point M to analyze the instantaneous cutting process. The force of the straw is shown in Figure 3. The support shovel provides an upward supporting force as the disc presses the straw against it, and the only force between the soil and the straw is the horizontal resistance F_w.

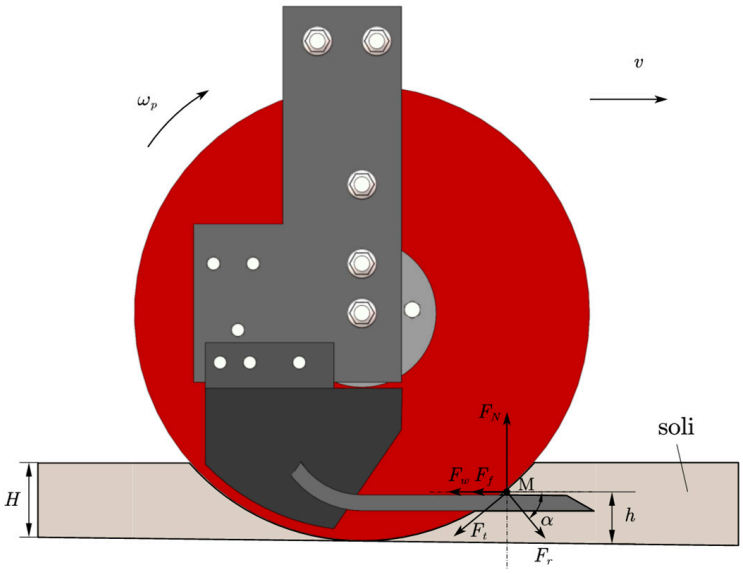

Figure 3. Analysis of straw force during the straw-cutting process: w_p is the rotational speed of the disc, rad/s; v is the forward speed of the operation, m/s; F_N is the support force of the support shovel on the straw, N; F_f is the friction force between the support shovel and the straw, N; F_w is the horizontal force between the soil and the straw, N; F_r is the positive pressure of the disc on the straw, N; F_t is the sliding shear force of the disc for the straw, N; α is the angle between the positive pressure of the disc on the straw and the horizontal plane of the soil, °; H is the depth of furrowing with disc openers, cm; h is the distance from the furrow bottom to the upper surface of the support shovel, cm.

According to the force analysis in Figure 3, the forces are balanced in all directions:

$$\begin{cases} F_r \sin\alpha + F_t \cos\alpha = F_N \\ F_w + F_f + F_t \sin\alpha = F_r \cos\alpha \end{cases} \quad (1)$$

where:

$$\begin{cases} F_t = F_r \tan \varphi_1 \\ F_f = F_N \tan \varphi_2 \end{cases} \tag{2}$$

In the formula, φ_1 is the friction angle between the disc cutter and the straw, °; φ_2 is the friction angle between the support shovel and the straw, °.

Take the diameter of the disc as D. There are

$$\alpha = \arcsin\left(1 - \frac{2h}{D}\right) \tag{3}$$

According to Formula (3), it is clear that when the value of D is determined, the larger h is, the smaller α is, and the straw is easier to push away by the disc at this time; when the value of h is determined, as the diameter D of the disc increases, α also increases, and the better the disc cuts the straw.

The support shovel and the disc are both constructed of 65Mn steel, which means that the values of φ_1 and φ_2 in Equation (2) are equivalent and should be taken as the same value φ. Organizing Equations (1)–(3) yields the following:

$$F_r = \frac{DF_w}{2\left[\left(1 - \tan^2 \varphi\right)\sqrt{Dh - h^2} - \tan \varphi (D - 2h)\right]} \tag{4}$$

According to previous research, the friction angle between maize straw and 65Mn steel typically ranges from 23 to 33° [19], and the friction angle between straw and soil is assumed to be 30° in this study. In the Huang-Huai-Hai region, winter wheat is typically planted 3 to 5 cm deep, with fertilizer depths ranging from 7 to 10 cm, vertical spacing distances between fertilizer and seed being greater than or equal to 5 cm [20], disc depth into the soil H set at 10 cm, and distance from the bottom of the furrow to the upper surface of the support shovel h set at 5 cm. According to Kushwaha's study [21], the optimal working diameter of the plane disc is 460 mm, which satisfies the agronomic criteria, and it is established that the disc diameter D is set at 460 mm.

The positive pressure F_r of the disc on the straw is a prerequisite to ensuring that the disc can cut off the straw. According to Equation (4), it can be seen that when the diameter of the disc, the friction angle between the straw and the steel plate, and the distance from the bottom of the groove to the upper surface of the support shovel are determined, the soil force F_w is the main factor affecting the cutting of the straw.

2.2.2. Force Analysis of the Support Shovel

The support shovel's tip first enters the soil, and as it advances, the soil will produce tillage resistance as the tip cuts through it. As the operating speed changes, the soil's shear strength will also change because the tip of the support shovel will cause the soil to be squeezed and deformed until it is crushed, which results in a dynamic change in the resistance. The support shovel moves through the soil at a uniform speed, assuming that the soil is homogeneous and isotropic. At this point, the tillage resistance is mostly seen in the soil's cohesion and pressure, as well as its friction with and adhesion to the support shovel [22]. Figure 4 depicts the force analysis of the supporting shovel in this condition.

The cohesion of the soil itself, the sliding friction force of the soil on the upper and lower surfaces, and the adhesion force of the soil to them must all be overcome throughout the advancing process of the support shovel [23]. So, the amount of tillage resistance P during cultivation can be expressed as follows:

$$P = (S + f_1 + T_1)\cos\beta + N_1 \sin\beta + (f_2 + T_2 + f_3 + T_3)\cos\varepsilon + (N_3 - N_2)\sin\varepsilon \tag{5}$$

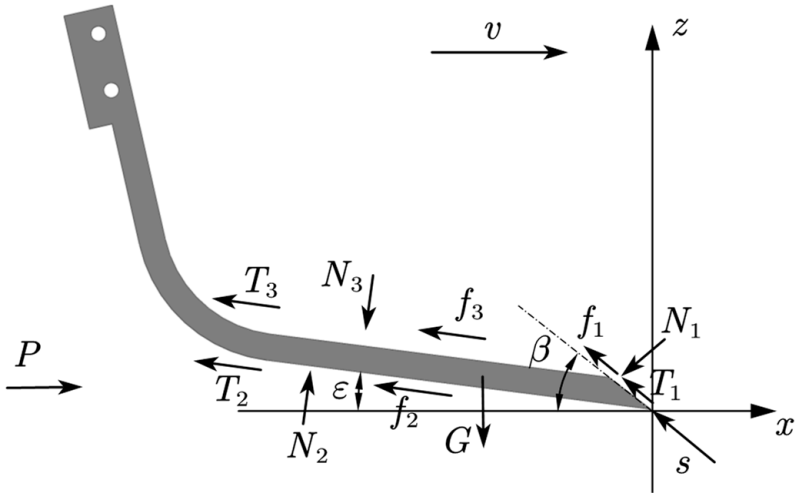

Figure 4. Force analysis of support shovel: P is the tillage resistance of the supporting shovel during tillage, N; S the soil cohesion, N; f_1, f_2, and f_3 are the soil's sliding friction forces on the edge, the shovel body's upper surface, and the bottom, respectively, N; N_1, N_2, and N_3 are the soil's normal pressures on the edge, the shovel body's upper surface, and the bottom, respectively, N; T_1, T_2, and T_3 are the soil's adhesion on the edge, the shovel body's upper surface, and the bottom, respectively, N; G is the gravity of the supporting shovel, N; β is the entry angle, °; ε is the entry gap angle, °.

Among them, the cohesion of the soil S is the force between soil particles that are bonded together as a result of molecular attraction; the strength of these forces varies depending on the soil's texture, structure, exchangeable cation composition, content of organic matter, content of soil water, etc. [24]. Better cohesiveness results in better resistance to tillage. The soil type, the physical characteristics of the soil, the material to which the soil adheres to the support plate, and the contact area are the main factors influencing the magnitude of the adhesion forces T_1, T_2, and T_3, with the soil moisture content having the largest impact on the physical characteristics of the soil [25]. The entry gap angle ε is related to the installation design of the support shovel, and the right entry gap angle can efficiently reduce soil entry resistance, facilitate soil cutting, and improve operational efficiency. The entry gap angle range of the common sliding opener is typically 0° to 12° [26], and it is important to consider both the function of the straw cutting and the design of the support shovel in order to determine the range of the entry gap angle of 0° to 5°. The entry angle β is related to the shape design of the shovel tip; the greater the entry angle, the more soil resistance the opener will encounter; on the other hand, the decrease will result in a loss of support shovel strength and shorten the shovel's useful life [27]. The entry angle is designed in reference to the entry angle of the common sliding opener, and the entry angle range of the common sliding opener is generally 25° to 55°; therefore, the entry angle takes the value range of 25° to 55° [28], and this paper is optimized by the discrete element method simulation of this parameter. The normal pressures N_1, N_2, and N_3 on the contact surfaces of the soil and the support shovel result in sliding friction forces f_1, f_2, and f_3, which are correlated with the friction angle between the soil and the furrow opener. When determining the friction angle, the sliding friction increases in proportion to the normal pressure on the contact surface, which, in turn, raises the resistance to plowing. Additionally, N_1, N_2, and N_3 are all connected to the combined impact of the soil's size, shape, and support shovel.

It can be shown that the soil moisture content is a significant element impacting the physical properties of the soil by analyzing the force during the work of the supporting shovel in the soil. The force of the soil on the straw is the main factor affecting the cutting of the straw, and the force of the soil on the straw is greatly affected by the physical properties of the soil, which is the conclusion reached after analyzing the force of the straw in the process of cutting the straw in the disc, so the soil moisture content also influences the

process of cutting straw. The force on the support shovel is mostly determined by the entry angle and entry gap angle, which also affect how much resistance the support shovel experiences. As a result, variables including soil moisture content, entry angle, and entry gap angle must be taken into account.

2.2.3. Design of the Support Shovel Structure

Figure 5 illustrates the structure of the support shovel. Decide on the main body's dimensions, which shall be 14 mm for the width b and 16 mm for the thickness c, to ensure that the support shovel has adequate strength. When cutting a straw with a disc and a support shovel, the length l should guarantee that the straw can be supported properly. At this time, $l > l_1 + d/2$, where the diameter of maize straw d is gradually increasing from the top down, measures the diameter of the straw's bottom, which ranges from 21 to 30 mm. Take the bottom of the diameter of the straw at the time of the largest value of 30 mm. The length of l_1 can be calculated by Formula (6), combined with Figure 5a substituting the relevant data that can be obtained l_1 = 181.1 mm; at this time, l > 196.1 mm. To prevent the straw from sliding out along the shovel tip, a margin of at least 10mm should be set. The design margin should be smaller than 50 mm since l is too lengthy to support the shovel's strength, and the length of l after rounding is between 206 and 246 mm. According to the support shovel arc section arc angle α_2 and the support shovel arc section arc radius r_1, the support shovel arc section in horizontal plane projection length l_2 can be calculated. Set the support shovel arc section arc angle α_2 for 70° and the support shovel arc section arc radius r_1 for 74 mm.

$$l_1 = \sqrt{\left(\frac{D+d}{2}\right)^2 - \left(\frac{D-d-2h}{2}\right)} \tag{6}$$

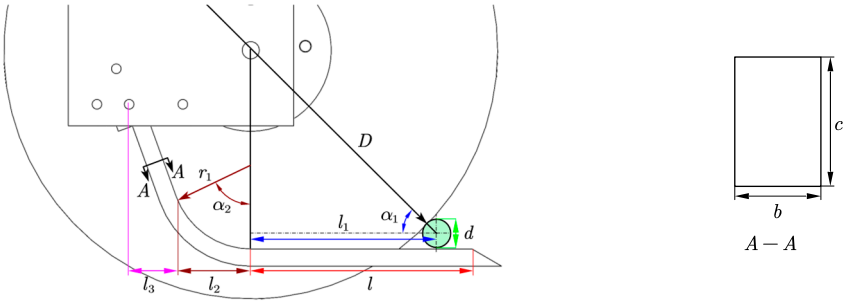

(**a**) Main view (**b**) Section view

Figure 5. Sketch of support shovel structure: l is the distance from the apex of the cutting edge of the support shovel to the vertical position of the center point of the disc, mm; l_1 is the distance from the center of the straw to the vertical position of the center point of the disc, mm; l_2 is the length of the circular arc section of the support shovel projected on the horizontal plane, mm; l_3 is the length of the tilted section of the support shovel projected on the horizontal plane, mm; d is the diameter of the straw, mm; r_1 is the radius of the arc of the circular arc section of the support shovel, mm; α_1 is the angle of the line connecting the center of the disc to the center of the straw and the plumb line, °; α_2 is the angle of the arc of the circular arc section of the support shovel, °.

Through the design of the support shovel structure, it is possible to draw the following conclusions: the appropriate shovel tip margin can prevent the straw from slipping out of the support shovel during the process of cutting straw with the support cutting disc, which is the key to making the support shovel play a supporting role and determines the effectiveness of the support shovel in cutting straw.

2.2.4. Design of Scraper

The disc cuts out slits in the soil, but because they are not wide enough for seeds to fall through, it is required to install auxiliary devices to make them wider. On the disc's

one side, soil can be compressed by the scraper to create the seed furrow. The scraper adopts an inclined structure with a narrow bottom and wide top, as shown in Figure 6. The lower part of the narrower is for the soil back to the gap reserved for the convenience of wet soil back to the seed furrow, so the lower periphery of the scraper is designed as a circular arc, the arc center and disc center coincide, in order to avoid the bottom of the furrow is too wide, the periphery of the scraper radius of the arc should be less than the radius of the disc, take r_2 = 220 mm. Winter wheat is typically planted 3 to 5 cm deep in the Huang-Huai-Hai region, with a furrow width of 40 mm, a disc thickness of 6 mm, a lower scraper e_1 scraper width of 34 mm, and an upper scraper e_2 scraper width of 40 mm. The scraper's length is too short, putting too much pressure on one side of the soil while also making it difficult to direct seeds. Its length is also too lengthy, which degrades the quality of the seed furrow that leads back to the soil and is recognized as l_4 = 199 mm.

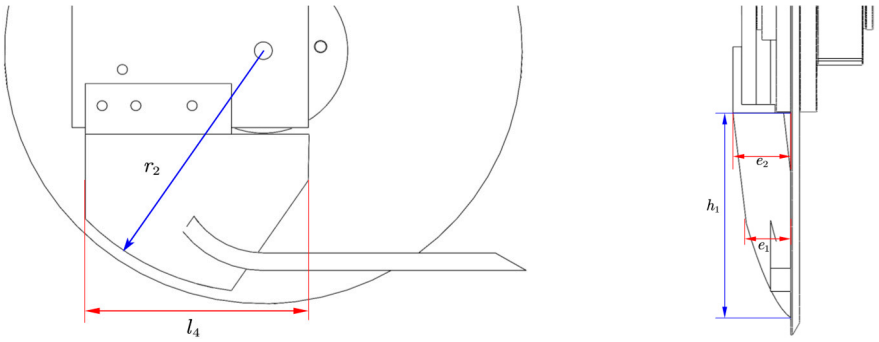

(**a**) Main view (**b**) Side view

Figure 6. Sketch of the scraper: l_4 is the length of the scraper, mm; r_2 is the radius of the peripheral arc of the scraper, mm; e_1 is the width of the lower part of the scraper, mm; e_2 is the width of the lower part of the scraper, mm; h_1 is the height of the scraper, mm.

Through the analysis above, the soil force on the straw is the primary element determining straw cutting, and the soil force on the straw is significantly influenced by the physical properties of the soil, of which the soil water content is a significant influence. The resistance of the support shovel in the movement and the support shovel in the design process are affected by the combined effects of soil moisture content, soil entry angle, soil clearance angle, and shovel tip margin.

2.3. Discrete Element Simulation of Furrow Openers

Due to the complexity of the motion involved in cutting straw with a disc in the soil, discrete element method simulation is a better method for simulating the interaction between the working parts and the soil as well as the straw [29]. The support-cutting "device–soil–straw" interaction model was developed using the discrete element simulation program EDEM in conjunction with the aforementioned analysis to simulate the working conditions of the support cutting device, identify the best parameter combinations for the support cutting device, and lay the groundwork for the ensuing field test.

2.3.1. Model of Support Cutting

Simulation test on the disc and support shovel. Set the soil simulation model's dimensions to 1500 mm in length, 360 mm in breadth, and 200 mm in height to ensure the operating range of the working parts. Creating a 3D geometric model in SolidWorks. This model was then saved in .step format and imported into the EDEM software. The device material was 65 Mn steel with a density of 7800 kg·m^{-3}, a shear modulus of 7.0 × 10^{10} Pa, and a Poisson's ratio of 0.3. The machine's forward speed is set to 0.83 m/s. The slip rate is low and negligible when the rotating speed of the disc is small [30]. The simulation can employ the active rotation of the disc in place of the passive rotation of the disc, and the disc is set to rotate periodically at 3.62 rad/s.

2.3.2. Model of Straw

The simulation test involves the disc cutting and crushing of straw. The maize straw is equivalent to an isotropic material, and the Hertz–Mindlin with bonding contact model in EDEM software is utilized to better represent the crushing state of straw. The parameters of maize straw in the literature [31,32] were used to set up the straw model. These parameters include the Poisson's ratio of straw, which is 0.40; its density, which is 470 kg·m^{-3}; its shear modulus, which is 1.7 × 10^6 pa; its contact model, which is the Hertz–Mindlin with bonding model, which sets the radius of the particles at 2 mm and the radius of the bonded disc at 3 mm; its normal stiffness per unit area, which is 9.6 × 10^6 N·m^{-3}; its shear stiffness per unit area, which is 6.8 × 10^6 N·m^{-3}; its critical normal stress, which is 8.72 × 10^6 Pa; and its critical shear stress, which is 7.5 × 10^6 Pa. The diameter of straw is taken to be 25 mm, the length is taken to be 180 mm, and the coefficient of restitution of the straw–straw contact is 0.49, the coefficient of static friction is 0.14, and the coefficient of rolling friction is 0.08; the coefficient of restitution of the contact between straw and 65 Mn steel is 0.66, the coefficient of static friction is 0.23, and the coefficient of rolling friction is 0.12, and the straw model is shown in Figure 7.

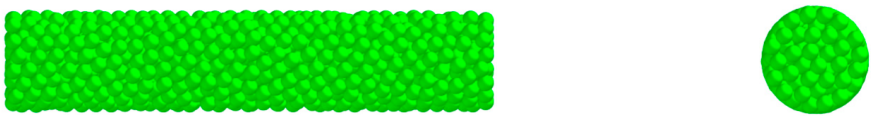

(**a**) Main view (**b**) Side view

Figure 7. Corn straw model.

2.3.3. Model of Soil

Considering that soil cohesion and adhesion are different in soil conditions with different water content, the soil is modeled with soil parameters of 12 ± 1%, 16 ± 1%, and 20 ± 1% water content, respectively, with reference to the literature [33]. The spherical particles with a radius of 4 mm were chosen to construct the soil model, and the particle contact model was the Hertz–Mindlin with bonding model. The model can be used to measure the soil's water content using the bonding radius and by modifying the bonding bonds' parameters to simulate the various soil properties [34], soil-related parameter references [31,33–40], and the precise simulation parameter settings, as shown in Table 1.

Table 1. Basic parameters of the soil model.

Parameters	Value		
Moisture content/%	12 ± 1	16 ± 1	20 ± 1
Density/(kg·m^{-3})	2050	2090	2150
Poisson's ratio	0.35	0.38	0.41
Shear modulus/Pa	0.85 × 10^6	1.05 × 10^6	1.24 × 10^6
Coefficient of restitution (soil–soil)	0.15	0.13	0.1
Coefficient of static friction (soil–soil)	0.532	0.364	0.268
Coefficient of rolling friction (soil–soil)	0.25	0.22	0.2
Normal stiffness per unit area/(N·m^{-3})	1.3 × 10^7	1.9 × 10^7	2.5 × 10^7
Shear stiffness per unit area/(N·m^{-3})	9 × 10^6	1.4 × 10^7	1.9 × 10^7
Critical normal stress/Pa	50,000	55,000	62,000
Critical shear stress/Pa	25,000	29,000	35,000
Coefficient of restitution (soil–straw)	0.6	0.5	0.4
Coefficient of static friction (soil–straw)	0.573	0.539	0.483
Coefficient of rolling friction (soil–straw)	0.21	0.18	0.16
Coefficient of restitution (soil–steel)	0.18	0.15	0.12
Coefficient of static friction (soil–steel)	0.351	0.571	0.65
Coefficient of rolling friction (soil–steel)	0.05	0.05	0.05
Bonded disk radius	4.34	4.47	4.62

2.3.4. Overall Model

Create a bed of particles to quickly generate the soil bin. In this procedure, maize straw is manufactured in the form of the particle factory API (Application Programming Interface), and the particle bonding time is set at 3.41 s. The soil layer is 200 mm thick in total, and the straws can be arranged in two different ways. The first one involves placing straw on the soil's surface to simulate the effect of straw being sliced by discs there. The second one involves placing straws in the middle and upper parts of the soil. The soil particles are divided into two layers, with the bottom layer being 150 mm tall, and the straw was laid on the surface of this layer, which was then covered with a 50 mm thick layer of soil to simulate the state of the straw when it is not cut off but is pressed into the soil and the support shovel just supports the straw. Four straws were placed in the soil bin, spaced 300 mm apart to reduce computational complexity, and the discrete element model is depicted in Figure 8.

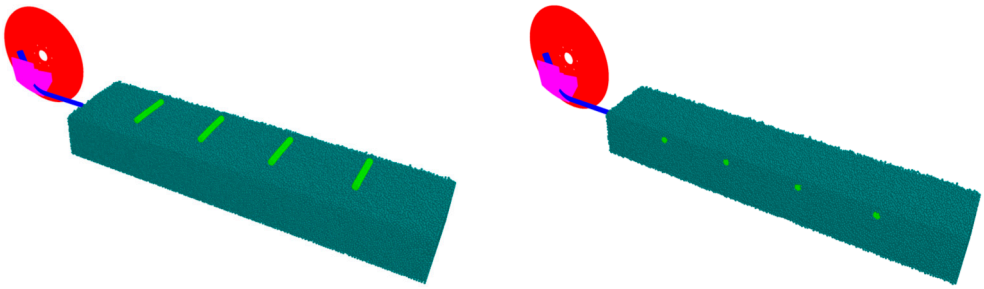

(**a**) Straw covers the soil surface (**b**) Straw in the upper-middle soil

Figure 8. Overall discrete element model.

2.3.5. Simulation Test Scheme

According to the previous analysis, the test factors were determined as follows: soil moisture content of 12 ± 1%, 16 ± 1%, and 20 ± 1%; entry angle of 25–55°; entry gap angle of 0–5°; and shovel tip margin of 10–50 mm. Among them, soil moisture content is an external factor, so a single-factor test is used to analyze its influence on the device in the process of cutting straw. The entry angle, the entry gap angle, and the shovel tip margin are the structural parameters in the design process of the device, so the quadratic orthogonal test is used to optimize the design of these factors. First, a single-factor simulation test using straw that was covered in soil was conducted to ascertain the impact of soil conditions with various moisture contents on the device for cutting straw. The soil moisture contents used were 12 ± 1%, 16 ± 1%, and 20 ± 1%, with entry angles of 25°, entry clearance angles of 0°, and shovel tip margins of 206 mm. Then, using the Design-Expert software for the entry angle, the entry gap angle, and the shovel tip margin of the multifactor simulation optimization test to determine the best parameter combinations for the high soil moisture content case, that is, simulating the soil moisture content of 20 ± 1%, the state of the straw after being pressed into the soil, with the entry angle of 25 to 55°, the entry gap angle of 0 to 5°, and the shovel tip margin of 10 to 50 mm.

2.3.6. Data Collection and Processing

The Number of Broken Bonds

The bond of the straw model will break during the simulation due to the action of shear stress. From the contact between the disc and the first straw to the last straw being completely cut off, the number of broken bonds with simulation time is a step-like regular change calculation of the length of each step change can be obtained by calculating the average time for the disc to cut off a straw. Figure 9 illustrates the bonds break regularity at 12% soil moisture content. The red dashed line denotes the moment when the disc first came into contact with the first straw, and the blue dashed line denotes the moment when the disc severed the first straw.

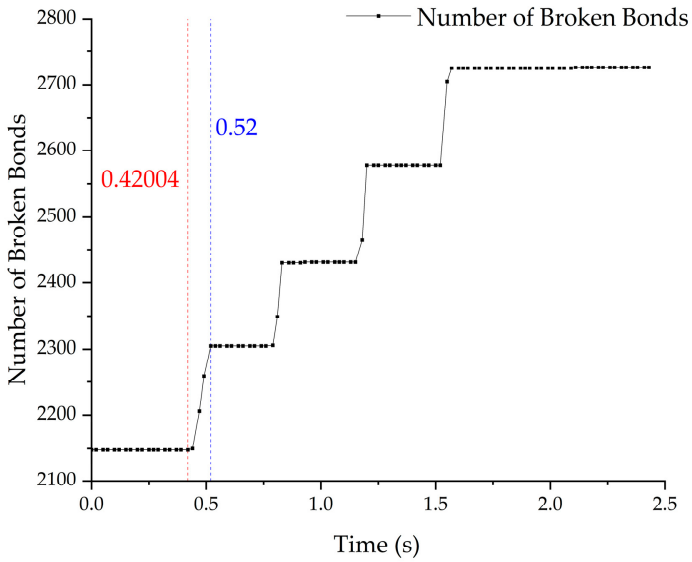

Figure 9. Number and time of broken bonds.

Tillage Component Resistance

After the simulation, the horizontal and vertical resistance of each component can be exported through the post-processing module of the software.

2.4. Field Experiment

2.4.1. Field Test Conditions and Equipment

On 15–18 November 2022, the test was conducted in Xinglongtun, Jiangshan Town, Laixi City, Qingdao City (36°36′17″ N, 120°36′50″ E). The test field was located in the wheat–maize double-ripening area of the Huang-Huai-Hai region, and the conservation-tillage model was practiced. The previous crop was maize at the time of the test, and the ground was covered in straw and stubble with an average moisture content of 35.21% for straw and roughly 17.82% for soil.

According to the optimal parameters obtained from the regression model, it is possible to complete the trial production of a single-disc furrowing and straw-cutting device. It is connected to the tractor by a three-point suspension during operation and is powered by a LUZHONG-1004A tractor, as shown in Figure 10a.

(**a**) Test equipment (**b**) Test conditions

Figure 10. Field experiment.

2.4.2. Test Indicators and Methods

Straw Cut-Off Rate

Twenty straws, each measuring approximately 55 cm in length, were distributed uniformly throughout the planting belt after the ground was cleared of any remaining straw (Figure 10b). The machine drives forward for a while before passing uniformly across the straw-laid planting belt under the conditions of 3 km/h forward speed and 100 mm furrow depth. After the operation, the straw was considered cut when it broke into two parts, and the rest was considered uncut. The total number of cut-off straws was counted, the cut-off rate of straws was calculated, the test was repeated three times, the average value was taken, and the cut-off rate was calculated by the formula:

$$\eta = \frac{Q_d}{Q_t} \times 100\% \tag{7}$$

where η is the straw-cutting rate, %; Q_d is the number of cut-off straws; Q_t is the total number of straws.

Stability Coefficient of Furrowing Depth

The test verified that the groove profile was opened by the furrow opener, as shown in Figure 11a (H_1 is the depth of the furrow opening). The measurement of furrow depth is shown in Figure 11b. When measuring the depth of the furrow, the method of taking the average value of segment measurement in the literature [41] was adopted, five points were randomly chosen to measure the furrow depth in the operating interval with the presence of straw, and the average value was obtained. The test was repeated three times, and the stability coefficient of the furrow depth was obtained by calculating the average and standard deviation of the furrow depth.

(**a**) Groove profile (**b**) Furrow depth measurement

Figure 11. Measurement of furrowing depth.

3. Results and Discussion

3.1. Single-Factor Simulation Test

3.1.1. Influence of Soil Moisture Content on the Number of Broken Bonds in Straw

The results of the single-factor simulation test are shown in Table 2. The largest number of bonds broken was 574 when the soil moisture content was 12 ± 1%, but the average time for a straw to be entirely cut was the shortest, 0.067 s. This shows that the soil was

hard and conducive for cutting straw when the soil moisture content was low. When the soil moisture content is 16 ± 1%, the number of broken bonds is 512, and the average time for a straw to be completely cut is 0.082 s. The least number of broken bonds occurs when the soil moisture level is 20 ± 1%. At this point, the average time required to entirely cut a stalk is 0.085 s, which is the longest time. The amount of time it took to completely cut off the straw increased as the soil's moisture content increased, indicating that as the soil's moisture content increased, the friction between soil particles and the straw decreased, making it more likely for the straw to slip on the soil's surface or go deeper into the soil. As a result, the disc had to move farther before the straw was completely cut off.

Table 2. Single-factor simulation test results.

Moisture Content/%	The Number of Broken Bonds	The Average Cut-Off Time/s
12 ± 1	578	0.067
16 ± 1	512	0.082
20 ± 1	505	0.085

3.1.2. Influence of Soil Moisture Content on the Device's Operational Resistance

The device is subjected to horizontal resistance in the direction of advance during the simulation process, as well as vertical resistance from the vertical, horizontal plane downward. The disc and support shovel were the analysis's objectives, and the resistance of the device was analyzed for various soil moisture contents.

The simulation lasts 2.43 seconds. The disc is assumed to finish contacting the first straw and entirely cut the last straw between 0.41 and 1.55 s, and this stage falls under the category of the disc cutting straw. Figure 12 shows the change curves of the resistance values.

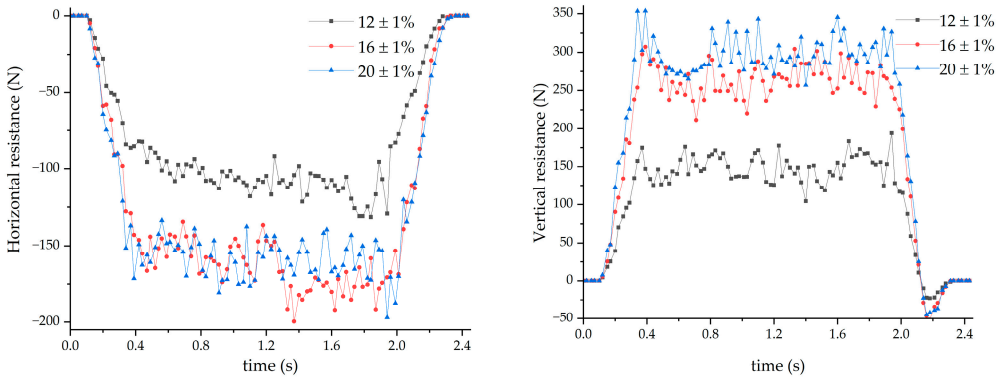

(**a**) Horizontal resistance (**b**) Vertical resistance

Figure 12. Variation in resistance values to discs under different soil moisture content conditions.

Figure 12a shows that as the disc is cutting straws, its horizontal resistance is negative, suggesting that the force acting in this direction is the opposite of the advancing direction. The horizontal resistance of the disc is low and steady, with a narrow fluctuation range when the moisture content is low, and the fluctuation range widens as the moisture content increases. The soil cohesion is less affected by the water content, and the disc's horizontal resistance is less sensitive to changes in water content when the water content is within a specified range.

Figure 12b shows that the vertical resistance to the disc during the stage of cutting straw by them was all positive, demonstrating that the disc was supported upward by the soil during its operation. When the water content of the soil is low, the overall vertical resistance of the disc is low. However, as the water content rises, the vertical resistance

significantly increases. This is likely because the viscous soil creates a buildup after the support shovel picks up the soil, which exerts more force on the disc.

The device was fully in the simulated soil bin from 0.6 to 1.83 s of the simulation period. The resistance to the support shovel during this time was analyzed, and Figure 13 shows the variation curve of the resistance value with the two green dashed lines denoting 0.6 and 1.83 s, respectively.

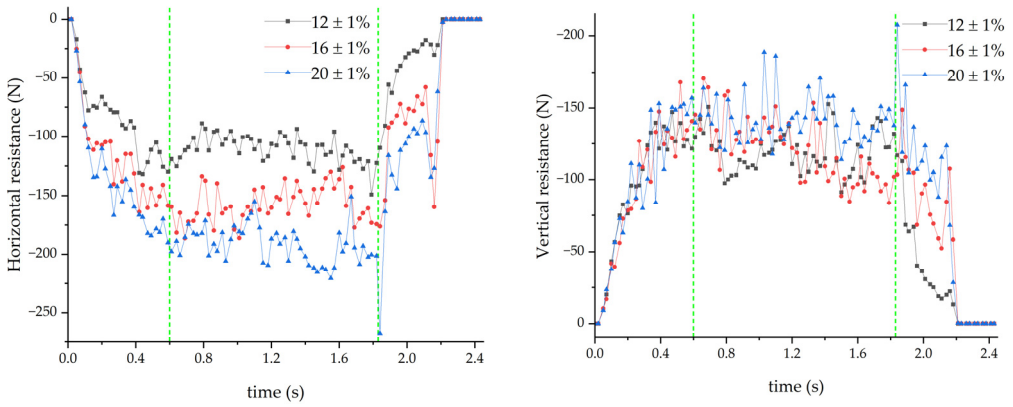

(**a**) Horizontal resistance (**b**) Vertical resistance

Figure 13. Variation in resistance values to support shovels under different soil moisture content conditions.

Figure 13a shows that the horizontal resistance to the support shovels is uniformly negative, showing that the force operates in the opposite direction to that of forward speed. When the soil moisture content is 12 ± 1%, the support shovel's horizontal resistance ranges from −88.94 to −149.04 N, with 149.04 N as the maximum value; when the soil moisture content is 16 ± 1%, the horizontal resistance ranges from −126.08 to −186.25 N, with 186.25N as the maximum value; and when the soil moisture content is 20 ± 1%, the horizontal resistance ranges from −150 to −220.66 N, with 220.66 N as the maximum value. The horizontal resistance and fluctuation range increase as the soil moisture content rises. This is because the soil's adhesion to the support shovel changes as the moisture content of the soil fluctuates. The soil's adhesion to the support shovel also increases as the moisture content increases, and as the soil and the support shovel generate relative sliding, tangential friction along the direction of movement rises as well, increasing the horizontal resistance of the support shovel.

Figure 13b shows that the vertical resistance of the support shovel is all negative, indicating that the support shovel is subjected to downward vertical resistance. When the soil moisture content is 12 ± 1%, the vertical resistance of the support shovel ranges from −91.21 to −152.68 N, with the maximum value of 152.68N; when the soil moisture content is 16 ± 1%, the vertical resistance ranges from −83.57 to −170.69 N, with the maximum value of 170.69N; when the soil moisture content is 20 ± 1%, the vertical resistance ranges from −113.94 to −188.94 N, with the maximum value of 188.94 N. The support shovel's vertical resistance is subjected to a wide range of fluctuations during the simulation process, but when the soil moisture content is 16 ± 1% and 20 ± 1%, the maximum resistance value is produced by a sudden change. The reason may be due to the increase in soil moisture content, so that the internal structure of the soil changes, the soil support for the straw may not be sufficient, the disc cannot quickly cut off the straw, the straw is pressed down and pushed forward, and when the soil is piled up to a certain extent, the straw that is between the disc and the soil layer on the upper part of the support shovel is cut off, resulting in a sudden change in resistance in the vertical direction.

3.2. Quadratic Orthogonal Simulation Test

3.2.1. Test Design

To find the optimal parameter, Design-Expert software was used to carry out a Box–Behnken test design for a total of 17 groups of experiments. The factor-level coding is shown in Table 3, and the experimental scheme and results are shown in Table 4, where X_1, X_2, and X_3 are the factor coding values, and the number of broken bonds Y is the experimental index.

Table 3. Coding table of the test factor level.

Levels	Entry Angle β/(°)	Entry Gap Angle ε/(°)	Shovel Tip Margin/mm
−1	25	0	10
0	40	2.5	30
1	55	5	50

Table 4. Experiment scheme and results.

Test Serial Number No.	Factors and Levels			Response Index
	X_1	X_2	X_3	The Number of Broken Bonds/Y
1	−1	−1	0	482
2	1	−1	0	505
3	−1	1	0	339
4	1	1	0	355
5	−1	0	−1	384
6	1	0	−1	412
7	−1	0	1	282
8	1	0	1	398
9	0	−1	−1	492
10	0	1	−1	367
11	0	−1	1	485
12	0	1	1	309
13	0	0	0	323
14	0	0	0	335
15	0	0	0	313
16	0	0	0	319
17	0	0	0	308

3.2.2. Analysis of Experimental Results and Establishment of Regression Model

The results of the simulation tests were analyzed by multiple fitting and regression analysis using Design-Expert data-processing software to obtain a regression model for the number of broken bonds Y. Table 5 shows the ANOVA results of the model. The regression model is significant, where X_1, X_2, and X_3 in the linear term and X_2^2 in the quadratic term were extremely significant ($p < 0.01$); X_1^2, X_3^2 in the quadratic term, and X_1X_3 in the interaction term were significant ($0.05 < p < 0.1$); and the rest of the terms were not significant. The three selected test factors have a quadratic relationship with the number of bond breaks, and the primary and secondary order of the degree of influence of each test factor on the test index Y is as follows: the entry gap angle, the entry angle, and the shovel tip margin. The non-significant terms were removed, and the fitting process was repeated to determine the regression mathematical model equation for the number of broken bonds Y:

$$Y = 319.6 + 22.88X_1 - 74.25X_2 - 22.63X_3 + 20X_1X_3 + 28.2X_1^2 + 72.45X_2^2 + 21.2X_3^2 \quad (8)$$

To further analyze the interaction effects of entry angle, entry gap angle, and shovel tip margin on the number of bond breaks Y, the response surfaces of the influencing factors on the test indexes were established, as shown in Figure 14. When the entry angle is

between 25° and 39°, as shown in Figure 14, the number of broken bonds tends to go lower as the shovel tip margin goes up. This is because the entry angle is smaller, the soil is disturbed less, the contact time between the straw and the disc is short, and the straw can be quickly severed. The entry angle is between 39° and 55°, and the number of broken bonds with the increase in the shovel tip margin was first reduced and then increased. This change is because the entry angle is small, the shovel tip margin on the number of broken bonds is greater than the entry angle, and the number of broken bonds is a reduction trend. Increased entry angle causes the support shovel to disturb the soil more, but it has less of an impact on the number of broken bonds than increased shovel tip margin, which causes more soil to warp ahead of time and advances the point at which the straw first makes contact with the disc and the support shovel. As the opener moves forward, the straw slides along the support shovel, increasing the time of the cutting of the straw, and the cutting surface of the straw produces tearing, which increases the number of broken bonds.

Table 5. Analysis of variance for the number of broken bonds.

Source	Sum of Square	Free Degree	Mean Square	*F* Value	*p* Value
Model	84,452.49	9	9383.61	30.72	<0.0001 **
X_1	4186.13	1	4186.13	13.70	0.0076 **
X_2	44,104.50	1	44,104.50	144.37	<0.0001 **
X_3	4095.13	1	4095.13	13.40	0.0081 **
X_1X_2	12.25	1	12.25	0.0401	0.8470
X_1X_3	1936.00	1	1936.00	6.34	0.0400 *
X_2X_3	650.25	1	650.25	2.13	0.1879
X_1^2	3348.38	1	3348.38	10.96	0.0129 *
X_2^2	22,101.06	1	22,101.06	72.35	<0.0001 **
X_3^2	1892.38	1	1892.38	6.19	0.0417 *
Residual	2138.45	7	305.49		
Lack of Fit	1711.25	3	570.42	5.34	0.0696
Pure Error	427.20	4	106.80		
Cor Total	86,590.94	16			

* means that the impact is significant ($0.01 \leq p < 0.05$); ** means that the impact is extremely significant ($p < 0.01$).

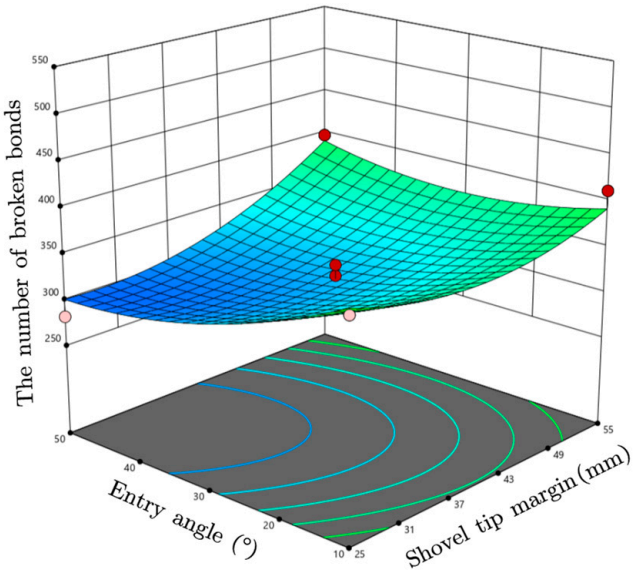

Figure 14. Influence of interaction factors on the number of broken bonds.

3.2.3. Parameter Optimization and Experimental Validation

A multi-objective optimization solution was performed on the entry angle, entry gap angle, and shovel tip margin based on the results of the response surface analysis and the actual operational requirements, using the numerical optimization function of the

Design-Expert software, with the aim of increasing the number of broken bonds. Then, specify the objective of the number of broken bonds Y to be maximized in the numerical module's criterion section. The constraint conditions of the objective function and each parameter variable are shown in Equation (9).

$$\begin{cases} \max Y(\beta, \varepsilon, l) \\ s.t \begin{cases} 25 \leqslant \beta \leqslant 55 \\ 0 \leqslant \varepsilon \leqslant 5 \\ 10 \leqslant l \leqslant 50 \end{cases} \end{cases} \tag{9}$$

The objective function is solved to obtain a variety of sets of optimum parameter combinations. At the entry angle of 49.44°, the entry gap angle of 0.05°, and the shovel tip margin of 10.10 mm, the number of straw bonds broken is 506. Round the optimal combination of parameters, set the entry angle at 49°, the entry gap angle at 0°, and the shovel tip margin at 10 mm, and run a simulation verification to obtain the number of broken bonds at 478. The number of broken bonds and optimization prediction of the results were obtained with a certain degree of difference. The difference between the two is 5.6%, which is small and meets the requirements of the operation.

3.3. Field Tests

The single-disc furrowing and straw-cutting device operates in the presence of straws, can cut off the surface straw, and produces a stable depth of the seed furrow. The results of the field test are provided in Tables 6 and 7, and the opener effect is displayed in Figure 15. As shown in Table 6, the average cut-off rate of the device was 71.7%. From Table 7, the stability coefficient of furrow depth for the device is 90.87%.

Table 6. Cut-off rate.

NO.	Total Number of Straws	Number of Straw Cut Off	Cut-Off Rate/%	Average Cut-Off Rate/%
1	20	15	75	
2	20	16	80	71.7%
3	20	12	60	

Table 7. Stability coefficient of furrowing depth.

NO.	H/mm	Average Value/mm	Standard Deviation	Coefficient of Variation/%	Stability Coefficient/%
1	10.44				
2	8.74	9.49	0.866	9.13	90.87
3	9.3				

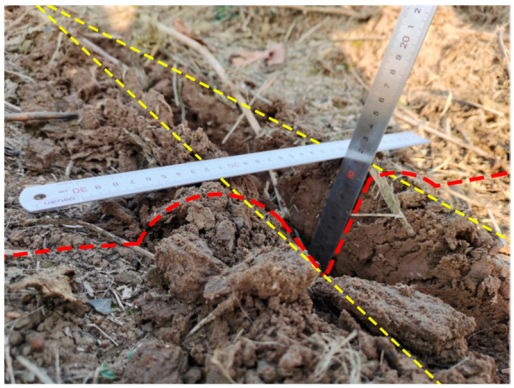

Figure 15. Effect of furrowing.

In the test process, if the straw is pulled by the disc out of the planting belt and the straw cannot be completely cut off by the disc, the cutting efficiency is reduced. The forward speed of the machine is also a significant factor affecting the efficiency of the disc opener in cutting the straw [9], and the test time when the forward speed of the machine is low also reduces the efficiency of the cutting of the straw. During the operation, it was difficult to keep the furrowing depth of the device stable. Due to the poor profiling ability of the device itself during the test, coupled with the influence of straw on the surface of the ground, it was difficult to improve the stability coefficient of the furrowing depth.

4. Conclusions

(1) A single-disc opener was created based on the principle of support cutting to address the issue of high soil moisture content, large amounts of straw, and the stubble-cutting device's inability to completely cut off the straw in the no-tillage sowing operation of wheat in the biannual ripening area of maize and wheat in the Huang-Huai-Hai region. The cutting mechanism of the device was revealed through the analysis of the force of the straw and the analysis of the device's performance.

(2) The "device-straw-soil" discrete element model was created, and a single-factor simulation test was conducted to examine the effects of soil conditions with different moisture contents on the number of broken bonds and the changes in resistance of the device to cut off the straw. A quadratic orthogonal test was conducted to establish a regression model for the number of broken bonds, and the following parameter combinations were found to be the most favorable: entry angle 49°, entry gap angle 0°, and shovel tip margin 10 mm.

(3) Results from field tests indicate that the average cut-off rate of the device on maize straw is 71.7%, and the stability coefficient of furrow depth is 90.87%, which shows that the machine has suitable operating performance and produces a stable depth of seed furrow.

Author Contributions: Conceptualization, G.Z. and H.L.; methodology, G.Z. and H.L.; software, Z.T. and D.H.; writing—original draft preparation, G.Z. and D.C.; writing—review and editing, J.H., Q.W., C.L. and C.W.; funding acquisition, H.L. All authors have read and agreed to the published version of the manuscript.

Funding: This research was funded by the China Agriculture Research System of MOF and MARA: CARS-03 and the 2115 Talent Development Program of China Agricultural University and Chinese Universities Scientific Fund: 2021TC105.

Institutional Review Board Statement: Not applicable.

Data Availability Statement: Not applicable.

Conflicts of Interest: The authors declare no conflict of interest.

References

1. Kassam, A.; Friedrich, T.; Derpsch, R. Global Spread of Conservation Agriculture. *Int. J. Environ. Stud.* **2019**, *76*, 29–51. [CrossRef]
2. He, J.; Li, H.; Chen, H.; Lu, C.; Wang, Q. Research Progress of Conservation Tillage Technology and Machine. *Trans. Chin. Soc. Agric. Mach.* **2018**, *49*, 1–19. [CrossRef]
3. Zhuang, J.; Jia, H.; Ma, Y.; Li, Y.; Di, Y. Design and Experiment of Sliding-knife-type Disc Opener. *Trans. Chin. Soc. Agric. Mach.* **2013**, *44*, 83–88. [CrossRef]
4. *ASABE Standard S477.1*; Terminology for Soil-Engaging Components for Conservation-Tillage Planters, Drills and Seeders. ASABE: St. Joseph, MI, USA, 2013.
5. Baker, C.J.; Saxton, K.E.; Ritchie, W.R.; Chamen, W.C.T.; Reicosky, D.C.; Ribeiro, F.; Justice, S.E.; Hobbs, P.R. *No-Tillage Seeding in Conservation Agriculture*, 2nd ed.; FAO: Rome, Italy, 2006.
6. Xu, G.; Xie, Y.; Peng, S.; Liang, L.; Ding, Q.S. Performance Evaluation of Vertical Discs and Disc Coulters for Conservation Tillage in an Intensive Rice–Wheat Rotation System. *Agronomy* **2023**, *13*, 1336. [CrossRef]
7. Torotwa, I.; Ding, Q.; Makange, N.R.; Liang, L.; He, R. Performance Evaluation of a Biomimetically Designed Disc for Dense-Straw Mulched Conservation Tillage. *Soil Tillage Res.* **2021**, *212*, 105068. [CrossRef]

8. Kumar, N.; Sawant, C.P.; Sharma, R.K.; Chhokar, R.S.; Tiwari, P.S.; Singh, D.; Roul, A.K.; Tripathi, S.C.; Gill, S.C.; Singh, G.P. Combined Effect of Disc Coulters and Operational Speeds on Soil Disturbance and Crop Residue Cutting under No-Tillage System in Soil Bin. *J. Sci. Ind. Res.* **2021**, *80*, 739–749. [CrossRef]
9. Zeng, Z.; Thoms, D.; Chen, Y.; Ma, X. Comparison of Soil and Corn Residue Cutting Performance of Different Discs Used for Vertical Tillage. *Sci. Rep.* **2021**, *11*, 2537. [CrossRef]
10. Ahmad, F.; Weimin, D.; Qishuo, D.; Hussain, M.; Jabran, K. Forces and Straw Cutting Performance of Double Disc Furrow Opener in No-Till Paddy Soil. *PLoS ONE* **2015**, *10*, e0119648. [CrossRef]
11. Magalhães, P.S.G.; Bianchini, A.; Braunbeck, O.A. Simulated and Experimental Analyses of a Toothed Rolling Coulter for Cutting Crop Residues. *Biosyst. Eng.* **2007**, *96*, 193–200. [CrossRef]
12. Bianchini, A.; Magalhães, P.S.G. Evaluation of Coulters for Cutting Sugar Cane Residue in a Soil Bin. *Biosyst. Eng.* **2008**, *100*, 370–375. [CrossRef]
13. Doan, V.; Chen, Y.; Irvine, B. Effect of Oat Stubble Height on the Performance of No-till Seeder Openers. *Can. Biosyst. Eng./Le Genie des biosystems au Canada* **2005**, *47*, 2.37–2.44.
14. Lu, C. Study on Anti-Blocking Technology and Device of Rotary Cuttingwith Slide Plate Pressing Straw for No-till Planter. Ph.D. Thesis, China Agricultural University, Beijing, China, 2014.
15. Sarauskis, E.; Masilionyte, L.; Romaneckas, K.; Kriauciuniene, Z.; Jasinskas, A. The Effect of the Disc Coulters Forms and Speed Ratios on Cutting of Crop Residues in No-Tillage System. *Bulg. J. Agric. Sci.* **2013**, *19*, 620–624.
16. Ahmad, F.; Weimin, D.; Qishou, D.; Rehim, A.; Jabran, K. Comparative Performance of Various Disc-Type Furrow Openers in No-Till Paddy Field Conditions. *Sustainability* **2017**, *9*, 1143. [CrossRef]
17. Murray, J.R.; Tullberg, J.N.; Basnet, B.B. *Planters and Their Components: Types, Attributes, Functional Requirements, Classification and Description (ACIAR Monograph No. 121)*; ACIAR: Canberra, Australia, 2006.
18. Malasli, M.Z.; Celik, A. Disc Angle and Tilt Angle Effects on Forces Acting on a Single-Disc Type No-till Seeder Opener. *Soil Tillage Res.* **2019**, *194*, 104304. [CrossRef]
19. Wang, Q.; Li, H.; He, J.; Lu, C.; Su, Y. Design and experiment on twist type ridge-clear device. *Trans. CSAE* **2010**, *26*, 109–113.
20. Ministry of Agriculture and Rural Affairs of the People's Republic of China. *Technical Specification for Mechanized Production of Wheat*; China Agriculture Press: Beijing, China, 2021. Available online: https://www.sdtdata.com/fx/fmoa/tsLibCard/183938.html (accessed on 23 July 2023).
21. Kushwaha, R.L.; Vaishnav, A.S.; Zoerb, G.C. Soil Bin Evaluation of Disc Coulters Under No-Till Crop Residue Conditions. *Trans. ASAE* **1986**, *29*, 40–44. [CrossRef]
22. Zhang, X.; You, Y.; Wang, D.; Wang, Z.; Liao, Y.; Lv, J. Design and Experiment of Soil-breaking and Root-cutting Cutter Based on Discrete Element Method. *Trans. Chin. Soc. Agric. Mach.* **2022**, *53*, 176–187. [CrossRef]
23. You, Y.; He, C.; Wang, D.; Wang, G. Interaction Relationship between Soil and Very Narrow Tine during Penetration Process. *Trans. Chin. Soc. Agric. Mach.* **2017**, *48*, 50–58. [CrossRef]
24. Lv, Y.; Li, B. *Soil Science*; China Agriculture Press: Beijing, China, 2006; pp. 73–75.
25. Wang, L.; Liao, J.; Hu, H.; Liu, L.; Bai, X.; Chen, C. Research status and prospect of adhesion reduction and desorption technology for agricultural machinery parts touching soil. *J. Chin. Agric. Mech.* **2021**, *42*, 214–221. [CrossRef]
26. Zhang, X.; Li, H.; Du, R.; Ma, S.; He, J.; Wang, Q.; Chen, W.; Zheng, Z. Effects of key design parameters of tine furrow opener on soil seedbed properties. *Int. J. Agric. Biol. Eng.* **2016**, *9*, 67–80. [CrossRef]
27. Chinese Academy of Agricultural Mechanization Sciences. *Agricultural Machinery Design Manual*; China Agricultural Science and Technology Press: Beijing, China, 2007.
28. Gou, W.; Ma, R.; Yang, W.; Fan, G.; Lei, X.; Hui, K.; Yang, H. Design of opener on no-till wheat seeder. *Trans. CSAE* **2012**, *28*, 21–25.
29. Ucgul, M.; Fielke, J.M.; Saunders, C. Three-Dimensional Discrete Element Modelling (DEM) of Tillage: Accounting for Soil Cohesion and Adhesion. *Biosyst. Eng.* **2015**, *129*, 298–306. [CrossRef]
30. Zhao, S.; Wang, J.; Yang, C.; Chen, J.; Yang, Y. Design and Experiment of Stubble Chopper under Conservation Tillage. *Trans. Chin. Soc. Agric. Mach.* **2019**, *50*, 57–68. [CrossRef]
31. Zhu, H.; Qian, C.; Bai, L.; Zhao, H.; Ma, S.; Zhang, X.; Li, H. Design and experiments of active anti-blocking device with forward-reverse rotation. *Trans. CSAE* **2022**, *38*, 1–11. [CrossRef]
32. Zhang, F.; Song, X.; Zhang, X.; Zhang, F.; Wei, W.; Dai, F. Simulation and experiment on mechanical characteristics of kneading and crushing process of corn straw. *Trans. CSAE* **2019**, *35*, 58–65. [CrossRef]
33. Zhao, S.; Liu, H.; Tan, H.; Cao, X.; Zhang, X.; Yang, Y. Design and performance experiment of opener based on bionic sailfish head curve. *Trans. CSAE* **2017**, *33*, 32–39. [CrossRef]
34. Pan, S.Q.; Cao, Z.F.; Jiang, S.S.; Yu, J.Q. Experimental Research on the Core Ploughshare Furrow Opener Based on the Discrete Element Method. In Proceedings of the 2014 International Conference on Mechanics and Civil Engineering (ICMCE 2014), Wuhan, China, 13–14 December 2014. [CrossRef]
35. Zhao, S.; Gu, Z.; Yuan, Y.; Lv, J. Bionic Design and Experiment of Potato Curved Surface Sowing Furrow Opener. *Trans. Chin. Soc. Agric. Mach.* **2021**, *52*, 32–42+64. [CrossRef]
36. Zhao, S.; Liu, H.; Yang, C.; Yang, L.; Gao, L.; Yang, Y. Design and Discrete Element Simulation of Interactive Layered Subsoiler with Maize Straw Returned to Filed. *Trans. Chin. Soc. Agric. Mach.* **2021**, *52*, 75–87. [CrossRef]

37. Tian, X.; Cong, X.; Qi, J.; Guo, H.; Li, M.; Fan, X. Parameter Calibration of Discrete Element Model for Corn Straw-Soil Mixture in Black Soil Areas. *Trans. Chin. Soc. Agric. Mach.* **2021**, *52*, 100–108+242. [CrossRef]
38. Sun, J. Structural and Mechanical Characteristics of Corn Stubble and Its Tribological Properties against Soil. Master's Thesis, Jilin Agricultural University, Changchun, China, 2011.
39. Li, J.; Tong, J.; Hu, B.; Wang, H.; Mao, C.; Ma, Y. Calibration of parameters of interaction between clayey black soil with different moisture content and soil-engaging component in northeast China. *Trans. CSAE* **2019**, *35*, 130–140. [CrossRef]
40. Zhao, S.; Liu, H.; Hou, L.; Zhang, X.; Yuan, Y.; Yang, Y. Development of deep fertilizing no-tillage segmented maize sowing opener using discrete element method. *Trans. CSAE* **2021**, *37*, 1–10. [CrossRef]
41. Jia, H.; Meng, F.; Liu, L.; Shi, S.; Zhao, J.; Zhuang, J. Biomimetic Design and Experiment of Core-share Furrow Opener. *Trans. Chin. Soc. Agric. Mach.* **2020**, *51*, 44–49+77. [CrossRef]